2018

Strategies for detecting biological molecules on Titan

Catherine Neish
cneish@uwo.ca

Ralph Lorenz
The Johns Hopkins University Applied Physics Laboratory

Elizabeth Turtle
The Johns Hopkins University Applied Physics Laboratory

Jason Barnes
The University of Idaho

Melissa Trainer
Goddard Space Flight Center

See next page for additional authors

Authors
Catherine Neish, Ralph Lorenz, Elizabeth Turtle, Jason Barnes, Melissa Trainer, Bryan Stiles, Randolph Kirk, Charles Hibbitts, and Michael Malaska

Strategies for detecting biological molecules on Titan

C.D. Neish[1], R.D. Lorenz[2], E. P. Turtle[2], J.W. Barnes[3], M. Trainer[4], B. Stiles[5], R. Kirk[6], C. A. Hibbitts[2], M. J. Malaska[5]

[1]Department of Earth Sciences, The University of Western Ontario, London, ON, N6A 5B7, Canada (Phone: 519-661-3188; E-mail: cneish@uwo.ca)
[2]The Johns Hopkins Applied Physics Laboratory, Laurel, MD 20723, USA
[3]Department of Physics, University of Idaho, Moscow, ID 83844, USA
[4]NASA Goddard Space Flight Center, Greenbelt, MD 20771, USA
[5]Jet Propulsion Laboratory, California Institute of Technology, Pasadena, CA, 91109, USA
[6]United States Geological Survey, Astrogeology Science Center, Flagstaff, AZ, 86001, USA

Research Paper resubmitted to Astrobiology

November 29, 2017

Running title: Detecting biomolecules on Titan

Abstract

Saturn's moon Titan has all the ingredients needed to produce "life as we know it". When exposed to liquid water, organic molecules analogous to those found on Titan produce a range of biomolecules such as amino acids. Titan thus provides a natural laboratory for studying the products of prebiotic chemistry. In this work, we examine the ideal locales to search for evidence of, or progression towards, life on Titan. We determine that the best sites to identify biological molecules are deposits of impact melt on the floors of large, fresh impact craters, specifically Sinlap, Selk, and Menrva craters. We find that it is not possible to identify biomolecules on Titan through remote sensing, but rather through in-situ measurements capable of identifying a wide range of biological molecules. Given the non-uniformity of impact melt exposures on the floor of a weathered impact crater, the ideal lander would be capable of precision targeting. This would allow it to identify the locations of fresh impact melt deposits, and/or sites where the melt deposits have been exposed through erosion or mass wasting. Determining the extent of prebiotic chemistry within these melt deposits would help us to understand how life could originate on a world very different from Earth.

Key words: Titan; Prebiotic chemistry; Solar system exploration; Impact processes; Volcanism

1. Introduction

Saturn's moon Titan has all the ingredients for life as we know it[1]. Titan's dense nitrogen-methane atmosphere supports a rich organic photochemistry (Hörst, 2017). Ultraviolet photons and charged particles dissociate the methane and nitrogen in the atmosphere to produce a suite of carbon, hydrogen, and nitrogen containing products ($C_xH_yN_z$), which eventually settle onto the surface. These products have been observed in Titan's atmosphere by the *Voyager* missions (Hanel et al., 1981; Kunde et al., 1981; Maguire et al., 1981) and in both the atmosphere and on the surface by the *Cassini-Huygens* mission (Niemann et al., 2005; Lavvas et al., 2008; Janssen et al., 2016).

Once on the surface, the products of Titan's photochemistry may react with liquid water in certain circumstances. Titan's surface is on average too cold for liquid water (~94 K – Fulchignoni et al., 2005), but transient liquid water environments may be found in impact melts and cryolavas (Thompson and Sagan, 1992; O'Brien et al., 2005; Neish et al., 2006). When organic molecules found on Titan's surface are exposed to liquid water, they quickly incorporate oxygen (Neish et al., 2008; 2009) to produce a range of biomolecules that include amino acids and possibly nucleobases (Neish et al., 2010; Poch et al., 2012; Cleaves et al., 2014). Impact melts and cryolavas of different volumes - and hence, different

[1] Here and throughout this paper, we use the term "life as we know it" to refer to carbon-based life that uses water as a solvent.

freezing timescales (O'Brien et al., 2005; Davies et al., 2010) - give us a unique window into the extent to which prebiotic chemistry can proceed over different time scales.

Thus, Titan provides a natural laboratory for studying the products of prebiotic chemistry. These products provide crucial insight into what may be the first steps towards life in an environment that is rich in carbon and nitrogen, as well as water. It is even possible that life arose on Titan and survived for a short interval before its habitat froze. Alternatively, life may have developed in Titan's subsurface ocean, and evidence of this life could be brought to the surface through geophysical processes such as volcanism (Fortes, 2000). A new exploration strategy is required to collect the results of these natural experiments; such measurements are not possible with the currently available data from the *Voyager* and *Cassini-Huygens* missions.

Even before *Cassini* reached the outer solar system, it was recognized that a post-*Cassini* scientific priority, especially for astrobiology, would be to access surface material for detailed investigation (Chyba et al., 1999; Lorenz, 2000). More recently, identifying "Planetary Habitats" was included as one of the three crosscutting themes of the National Research Council's "Visions and Voyages for Planetary Science in the Decade 2013-2022" (Space Studies Board, 2012). In addition, Titan is currently listed as one of six potential mission themes for NASA's next New Frontiers mission[2]. Such a mission could be specifically designed to identify the products of prebiotic chemistry on Titan's surface.

In this work, we determine the ideal locales to search for biomolecules on Titan, and suggest mission scenarios to test the hypothesis that the first steps towards life have already occurred there. In this scenario, we would consider a substantial presence of biomolecules (i.e., compounds that are essential to life as we know it) as either a compelling indicator of an advanced prebiotic environment or as a possible sign of extinct (or more speculatively, extant) life.

2. Geological settings for aqueous chemistry on Titan

Liquid water is both a crucial source of oxygen and a useful solvent for the generation of biomolecules on Titan's surface. Thus, if we wish to identify molecular indicators of prebiotic chemistry on Titan, we need to determine where liquid water is most likely to have persisted. Although Titan's average surface temperature of ~94 K precludes the existence of bodies of liquid water over geologic timescales (unless there is an active hotspot – see Schulze-Makuch and Grinspoon, 2005), it does not rule out the presence of water on the surface for short periods of time. We are likely to find transient liquid water environments on the surface of Titan in two distinct geological settings: (1) cryovolcanic lavas and

[2] See https://newfrontiers.larc.nasa.gov.

(2) melt in impact craters. In addition, Titan's deep interior has a liquid water layer perhaps hundreds of kilometers thick, which may also contain biomolecules (Fortes, 2000; Iess et al., 2012). Samples of this ocean may be transported to the surface through cryovolcanic processes before eventually freezing. Thus, if we wish to find biomolecules on the surface of Titan, we should focus our search in and around cryovolcanoes and impact craters.

2.1 Cryovolcanoes

On Titan, lavas are generally referred to as cryolavas, since they involve the eruption of substances that are considered volatiles on the surface of Earth (e.g., water, water-ammonia mixtures, etc.). Features suggested to be caused by cryovolcanism were first discovered on the icy satellites during the *Voyager* missions (e.g., Jankowski and Squyres, 1988; Showman et al., 2004). More recent observations point to the existence of present-day activity on Enceladus (Porco et al., 2006) and Europa (Roth et al., 2014; Sparks et al., 2017).

Two conditions must be met for cryovolcanic flows to be present on a surface: liquids must be present in the interior and those liquids must then migrate to the surface. Theoretical models of Titan's formation and evolution predict that a substantial liquid water layer must still exist in its interior, provided a sufficient amount of ammonia is present in the ocean (Tobie et al., 2005). Observations by the *Cassini* mission have confirmed the presence of a liquid water subsurface ocean. Measurements of the tidal love number by the Radio Science experiment require that Titan's interior is deformable over its orbital period, consistent with a global ocean at depth (Iess et al., 2012). In addition, the Permittivity, Wave and Altimetry instrument on ESA's *Huygens* probe detected a electric current in Titan's ionosphere, consistent with a Schumann resonance between two conductive layers. The lower layer was estimated to lie 55-80 km below the surface, suggestive of a salty, subsurface ocean (Béghin et al., 2012). Other analyses of Titan's overall shape, topography, and gravity field are consistent with an ice shell of this thickness overlying a relatively dense subsurface ocean (Nimmo and Bills, 2010; Mitri et al., 2014)

The second requirement for cryovolcanism is for liquid to be transported from the interior to the surface. One plausible way to transport lava is through fluid-filled cracks. Mitri et al. (2008) proposed a model in which ammonia-water pockets are formed through cracking at the base of the ice I shell. As these ammonia-water pockets undergo partial freezing, the ammonia concentration in the pockets would increase, decreasing the negative buoyancy of the ammonia–water mixture. Unlike pure liquid water, a liquid ammonia-water mixture of peritectic composition (ρ = 946 kg m^{-3}) is near-neutral buoyancy in ice (ρ = 917 kg m^{-3}) (Croft et al. 1988). Though these pockets could not easily become buoyant on their own (given the difference in density of ~20-30 kg m^{-3}), they are sufficiently close to the neutral buoyancy point that large-scale tectonic stress patterns (tides, non-synchronous rotation, satellite volume changes, solid state convection, or subsurface pressure gradients associated with topography) could enable the ammonia-water to erupt effusively onto the surface. Evidence of such stress patterns are observed on Titan (Cook-Hallet et al., 2015; Liu et al., 2016). Any lava extruded in this way would likely have a peritectic composition near that of pure ammonia dihydrate (33 wt. % ammonia).

We can test the hypothesis that cryolavas have erupted onto Titan's surface by looking for morphological constructs on the surface consistent with volcanism. The *Cassini* RADAR instrument has imaged approximately two-thirds of the surface of Titan, producing views of the landscape with resolutions as good as 350 m. Although it is difficult to conclusively identify cryovolcanic constructs at these resolutions (Moore and Pappalardo, 2011), several features remain difficult to explain through any other geologic process (Lopes et al., 2013). The most intriguing of these features is Sotra Patera (part of a region formerly known as Sotra Facula). This region includes the deepest pit and some of the highest mountains on Titan, as well as the associated flow-like features of Mohini Fluctus, a 200 km feature extending from Sotra Patera with a lobate edge (Figure 1). If Sotra Patera is indeed a volcanic construct, the lava flows there would be an interesting location for studying the interaction of liquid water with organic molecules on Titan's surface.

However, unless this region represents a persistent hot spot, it is unlikely that the lava will remain liquid long enough for aqueous chemistry to produce complex, biological molecules. (Thus far, no evidence of hot spots has been observed on Titan – Lopes et al., 2013.) Flow lobes tens of meters thick in Mohini Fluctus (Lopes et al., 2013) would likely cool over relatively short timescales: if heat is lost only by conduction, the one-dimensional thermal conduction equation predicts that it should take only one year for a ten-meter-thick flow of water or ammonia dihydrate to completely freeze. Even a 200 m high cryovolcanic dome that is 90 km in radius is expected to take only several hundred years to freeze completely (Neish et al., 2006).

In addition, if these lavas have a peritectic composition close to that of pure ammonia dihydrate, they would erupt close to a temperature of 176 K. This would significantly affect reaction rates. In a 13 wt. % ammonia solution at 253 K, reactions between Titan haze analogues and ammonia-water have half-lives of a few days (Neish et al., 2009). According to the Arrhenius equation, a reaction at 253 K with an activation energy of 50 kJ/mol would take 3 x 10^4 times longer in a peritectic melt at 176 K. Thus, a reaction that took a few days to complete at the higher temperature would take a few hundred years to complete at the lower temperature. The aqueous chemistry in cryolavas may not have sufficient time or energy to produce more complicated prebiotic molecules.

More speculatively, Titan's subsurface ocean may contain biomolecules, or even simple life forms (Fortes, 2000). Evidence of such biology could be found frozen in the cryovolcanic lavas on the surface of Titan. However, given the uncertain presence of biomolecules in the subsurface ocean, and the challenges inherent in transporting material to the surface, we judge the priority for exploration should focus on another geologic setting where biomolecules are more likely to be present: impact melt deposits.

2.2 Impact craters

When a comet or asteroid impacts a planet, energy becomes available to melt its surface. Ponds and flows of melted crustal rock are observed in and around impact craters on terrestrial planets (e.g. Hawke and Head, 1977). Models suggest that melt should be produced on icy satellites as well (Pierazzo et al., 1997; Artemieva and Lunine 2003; Kraus et al. 2011) and smooth regions at the center of the largest craters on Ganymede have been interpreted to be solidified impact melt (Jones et al., 2003; Bray et al., 2012).

Titan's atmosphere is capable of shielding the surface from smaller impactors (Ivanov et al., 1997; Artemieva and Lunine, 2005; Korycansky and Zahnle, 2005), so any projectile that does strike the surface must necessarily be large. Such impactors would melt a substantial amount of Titan's crust. Artemieva and Lunine (2003) conducted three-dimensional hydrodynamical simulations of impacts into Titan's crust, and found that a 2 km icy projectile entering the atmosphere at an oblique angle with a velocity of 7 km/s would generate 2-5 % melt by volume within a transient crater 10-25 km in diameter. The amount of melt increases with impact energy, so larger craters would contain a larger percentage of melt by volume (Grieve and Cintala, 1992; Cintala and Grieve, 1998; Elder et al., 2012).

This melt could collect in the lowest parts of the crater, forming a sheet several hundred meters thick. Given the higher density of liquid water compared to the density of ice I, some melt could also drain into fractures in the crater floor before freezing, forming the central pit features seen in craters on many icy satellites (Elder et al., 2012). Using fracture volumes estimated from the gravity anomalies observed over terrestrial impact craters, and assuming flow through plane parallel fractures, Elder et al. (2012) estimated that melt will be retained for Titan craters with diameters greater than ~90 km. However, this is a somewhat idealized situation; in reality, fractures in the brecciated floor of an impact crater are much more sinuous, with variable direction and width. If the fractures have a tortuosity of two, only ~1/3 as much melt would drain (Elder et al., 2012). (Tortuosity is the ratio of the length of the fracture to the depth of the fractured region.) In addition, it is likely that fractures do not have a constant width, which would cause the flow to slow through narrower passages, reducing the total amount of melt volume drained. Since larger craters produce a larger fraction of melt by volume than smaller craters (Grieve and Cintala, 1992), a reduced drainage efficiency means that melt could also be retained for somewhat smaller impact craters on Titan (larger craters would simply retain more melt than they would if there was more efficient drainage).

The organics found on Titan's surface could then react with melt present on the crater floor, in its ejecta blanket, or perhaps mixed with melt that drains into fractures. Artemieva and Lunine (2003) found that a significant fraction (10%) of Titan's organic surface layer would be only lightly shocked in an impact. As a result, these organic molecules would be only partially altered, providing reactants for any subsequent aqueous chemistry. In impact craters on Earth, impact melt often incorporates large amounts of clastic material from non-melted, but shocked target rocks (Osinski et al., 2017), suggesting there would be efficient mixing between liquid water and organic clasts on Titan. In this way, impact melts could provide "oases" for prebiotic chemistry to occur on Titan's surface.

Once melted by the impact, any liquid water generated would begin to cool to the ambient temperature of ~94 K. Thompson and Sagan (1992) were the first to estimate the lifetime of melt pools generated in impacts on Titan. They approximated the melt as a buried sphere of water freezing inward, and found lifetimes of $\sim 10^4$ yr for a 10 km diameter crater, and $\sim 10^6$ yr for a 100 km diameter crater. O'Brien et. al. (2005) refined the calculation using a thermal conduction code, including more realistic geometries (such as sheets of melt several hundreds of meters thick) and the possibility of water-ammonia melt mixtures. With the melt fraction calculated by Artemieva and Lunine (2003), they found somewhat shorter lifetimes of ~10^2-10^3 yr for a 15 km diameter crater, and ~10^3-10^4 yr for a 150 km diameter crater. These lifetimes are considerably longer than those for lava flows tens of meters thick, allowing more time for aqueous chemistry to proceed. (Lifetimes could be reduced if a significant proportion of the melt were to drain into the bottom of the crater, as discussed above.)

Impact melts would provide an excellent medium for aqueous chemistry on Titan. In addition to having longer freezing timescales than cryovolcanic flows, they are also likely to be emplaced at much higher temperatures. Melted crustal rock (as opposed to water extruded from depth) is more likely to yield a water-rich composition, with temperatures near the water liquidus (273 K), not the ammonia-water peritectic (176 K). Temperatures may even exceed the liquidus initially, given the large amounts of energy available from an impact. For example, there is evidence for super-heating of several hundred Kelvins in impact melts on Earth (Horz, 1965; El Goresy, 1965) and the Moon (Simonds et al., 1976). This could increase the temperature of the melt above the liquidus, accelerating the chemistry occurring in the melt ponds. Reactions between Titan haze analogues and liquid water were roughly 20 times faster at 40°C than at 0°C (Neish et al., 2008).

How many craters are available for such chemistry on Titan? We expect impact cratering to be an important process in the Saturnian system, whose satellites retain thousands of scars from past impacts (e.g., Kirchoff and Schenk, 2010). Before *Cassini* arrived at Saturn, the cratering history on Titan was unknown from direct observations, so estimates of the cratering rate were made by extrapolating the crater distributions observed on other Saturnian satellites, or by predicting impact rates by comet populations. Such estimates suggested that at least several hundred craters larger than 20 km in diameter should be present on Titan (Zahnle et al. 2003). Now that *Cassini* RADAR has been able to observe Titan's surface, an extreme paucity of craters is observed. Only 23 certain or nearly certain craters and ~10 probable craters have been observed on Titan in this size range, with a handful of smaller crater candidates (Wood et al., 2010; Neish and Lorenz, 2012; Neish et al., 2016). This population has crater depths consistently shallower than similarly sized fresh craters on Ganymede, suggestive of extensive modification by erosion and burial (Neish et al., 2013). Although aeolian infilling appears to be the dominant modification process on Titan, fluvial erosion seems to play an important secondary role (Neish et al., 2016). In addition, there is an almost complete absence of craters near Titan's poles, which may be indicative of marine impacts into a former ocean in these regions (Neish and Lorenz, 2014) or an increased rate of fluvial erosion (Neish et al., 2016).

We therefore judge that the best targets for observing the products of aqueous – and possibly biological – chemistry on Titan are the floors of large, relatively fresh impact craters. Fresh impact craters on Titan are subject to a minimal amount of fluvial incision (which would expose the core of any impact melt sheet), but little to no burial by sand or sediments (Neish et al., 2016). These structures will contain the largest amount of impact melt, and that melt will be easier to access with a spacecraft than the melt in more degraded craters (where it is likely buried under a thick deposit of sediment).

To determine the best candidates for such studies, we consider the relative degradation states of all ‘certain’ or ‘nearly certain’ craters on Titan with diameters greater than 75 km (i.e., those craters most likely to retain impact melt). As in Neish et al. (2013), we quantify the degradation state of a crater by considering the relative depth of a Titan crater compared to a fresh, unmodified crater on Ganymede with a similar diameter. The relative depth, R, is given by $R(D) = 1 - d_t(D)/d_g(D)$ where $d_t(D)$ is the depth of a crater with diameter D on Titan, and $d_g(D)$ is the depth of a crater with diameter D on Ganymede. A relative depth of zero indicates the crater has the same depth as a crater on Ganymede and is thus unmodified by erosion; a relative depth of one indicates the crater is completely flat.

There is topography data for seven craters on Titan with D > 75 km. The relative depths of five of these craters were previously reported in Neish et al.

(2013) and Neish et al. (2015). Topography data for the sixth crater – the ~80 km diameter Selk crater – was obtained during *Cassini*'s T95 pass of Titan on 14 October 2013 (Figure 2a). A topographic profile was acquired through the center of the crater using the SARTopo technique (Stiles et al., 2009). We calculated depth, $d = h_1 - h_2$, by taking the difference between the highest point on the crater rim and the lowest point on the crater floor, on both sides of the crater, d_1 and d_2 (Figure 2b). Systematic errors in height, dh_i, were propagated throughout the analysis. These errors were determined from radar instrument noise and viewing geometry (Stiles et al., 2009). Using this technique, the depth of Selk is 470 ± 90 m.

Topography data for the seventh crater – the ~140 km diameter Forseti – was generated from stereo topography produced from overlapping radar images from the T23 and T84 passes of Titan. Unfortunately, the stereo pair only covers the northeast corner of the crater, so our depth estimate is based solely on the rim heights and floor depths observed in this quadrant (Figure 3a). The floor elevation is -2144 ± 35 m and the rim elevation is -1963 ± 54 m, for an average depth of 180 ± 60 m. In addition, there is a SARTopo profile through the northeast portion of the crater, generated using data from *Cassini*'s T23 pass (Figure 3b). Unfortunately, there is a data gap present on the crater floor, so we are only able to calculate a minimum crater depth using this data set (Figure 3c). Using the same technique as described for Selk, we found a *minimum* crater depth of 410 ±

50 m. This differs significantly from the depth derived from the stereo pair.

There are several possible reasons for this discrepancy. The crater floor may appear to be level with the crater rim in the stereo pair due to a lack of features on the floor. Identifiable features present in both images are necessary to make stereo measurements. This situation could cause elevations on the crater floor to be interpolated from the nearest rim points, artificially raising points on the crater floor in the stereo data. In addition, impact craters often have large variations in rim height (see, for example, Neish et al. 2017). By only measuring one quadrant of the crater rim, we may not be getting a representative sample of the rim height, thus biasing our result by using a lower than average portion of the crater rim for depth measurements.

Updated topography data are also available for the ~100 km diameter Hano crater. The data were generated from stereo topography produced from overlapping radar images from *Cassini*'s T16 and T84 passes of Titan, and cover more than half of the crater from the southwest quadrant to the northeast quadrant. The result shows a crater with little noticeable topography (Figure 4a). In fact, the average heights in the rim region (-1500 ± 170 m) and the average heights in the floor region (-1510 ± 140 m) are nearly identical, suggesting that Hano crater is essentially flat (R ~ 1). The initial depth estimate (d = 525 ± 100 m) by Neish et al. (2013) using SARTopo only took into consideration one profile across the southernmost rim of the crater, so it is possible that profile was not representative of the crater as a whole. An updated SARTopo profile is now available, covering both the northern and southern rim of Hano crater (Figure 4b). Using the same technique as described for Selk, we found a new crater depth of 420 ± 40 m (Figure 4c). As with Forseti, the stereo and SARTopo values differ considerably for Hano crater, possibly for the same reasons outlined above. However, both of the newly derived depths are lower than the initial estimate from Neish et al. (2013). Thus, Hano appears to be more degraded than originally suggested, which is consistent with its observed morphology in the RADAR data (Wood et al., 2010).

We summarize the relative depths of the seven craters in Table 1. Of these, only two have relative depths < 0.6 for all current topography measurements: Sinlap and Selk. We judge these to be the least degraded craters in this size range. In terms of relative depth, Sinlap would be considered the 'freshest' crater on Titan, with $R = 0.4 \pm 0.2$. It is difficult to assess the relative depth of the largest crater on Titan, Menrva, since craters in this size range ($D >$ 150 km) on icy satellites are associated with a sharp reduction in crater depth and anomalous impact morphologies (Schenk, 2002). However, given the large amount of impact melt expected in such a large crater, it remains a high priority target for future exploration. The craters of interest are shown in Figure 5.

3. Identifying biological molecules on Titan

To identify biological molecules on Titan, it will be necessary to obtain more detailed data than are currently available from past ground- and space-based observations. As we describe below, the remote sensing data sets lack the spatial and spectral resolution to make definitive conclusions about the composition of Titan's surface. Compositional information regarding the potential presence of biological molecules could be obtained from in-situ observations, but only if (a) the associated instrumentation is designed for such a task, and (b) the surface material can be obtained from the targeted regions described in Section 2. In this section, we describe the difficulties in assessing surface composition remotely, and describe possible approaches for in-situ detection of biological molecules.

3.1 Detection by remote sensing?

To date, Titan has been a focus of a number of spacecraft missions, as well as numerous Earth-based telescopic observations. The collected data have provided global observations of Titan's atmosphere and surface at a range of spatial and spectral resolutions. However, it has remained a difficult challenge to determine the composition of Titan's surface from remote observations (Hörst, 2017), for reasons we expand upon below.

Pioneer 11 was the first spacecraft to encounter Saturn, and acquired the first near range images of Titan in 1979 (Tomasko, 1980). This set the stage for the *Voyager* missions, which flew by Saturn and Titan in 1980 (*Voyager* 1) and 1981 (*Voyager* 2), respectively (Stone, 1977). The *Voyager* missions returned important information about Titan's atmospheric chemistry (e.g., Hanel et al., 1981; Kunde et al., 1981; Maguire et al., 1981; Yung et al., 1984), but the cameras on *Voyager* were unable to resolve any of the fine details of the surface (Richardson et al. 2004). Such images were not obtained until the *Cassini-Huygens* mission entered orbit around Saturn in 2004. Over the past thirteen years, the *Cassini* RADAR, VIMS (Visual and Infrared Mapping Spectrometer), and ISS (Imaging Science Subsystem) instruments have provided our first detailed looks at the surface of Titan (Elachi et al., 2005; Barnes et al., 2005; Porco et al., 2005), with the RADAR instrument providing the highest resolution views. However, only ~2/3 of Titan's surface was imaged by the RADAR instrument by the end of the Cassini mission, at resolutions of 350 - 2000 m. This limited spatial resolution impacts our ability to differentiate surface units on Titan, and hence, determine their differing compositions.

In addition to the limited spatial resolution available for Titan, there is limited spectral resolution available for compositional analysis. Due to the presence of Titan's thick nitrogen-methane atmosphere, remote spectroscopic measurements are restricted to a discrete number of atmospheric 'windows', where scattering and/or absorption are reduced (Lorenz and Mitton, 2002). For example, the VIMS instrument on *Cassini* has only been able to image the surface of Titan at seven atmospheric windows at wavelengths ranging between 0.94 and 5 µm (Brown et al., 2004).

High spectral resolution is crucial for the remote identification of surface materials. The observation of key spectral features has provided essential information about the composition of many planetary bodies, including the identification of water ice on the Galilean satellites (Pilcher et al., 1972), carbonates on Mars (Ehlmann et al., 2008), and hydroxyl on the Moon (Pieters et al., 2009; Clark, 2009; Sunshine et al., 2009). With only a handful of wavelengths available for surface analysis, similar identifications may be impossible on Titan. The observations are further complicated by residual absorption and scattering within Titan's atmospheric windows. For example, Hayne et al. (2014) found strong atmospheric attenuation in the 2.7 µm window compared to the 2.8 µm window, resulting in a reversal of the spectral slope expected for water ice.

These limitations are present for both orbital and aerial platforms (such as a balloon or aircraft). This is true even though the amount of atmospheric absorption between an aerial platform and the surface is much less than that encountered by an orbiter. For example, the Huygens probe was able to image Titan's surface at the meter scale from an altitude of 10 km (Tomasko et al., 2005), but surface spectra could not be obtained outside of a few specific spectroscopic windows (Tomasko et al., 2005). This is because at these altitudes, there is little solar illumination for the surface to reflect, since much of the sunlight has been absorbed or scattered by the overlying atmosphere (Tomasko et al., 2005). McDonald et al. (2015) modeled the effect of methane absorption with altitude, and found a slight widening of the spectral windows at altitudes closer to the surface. However, they neglected to include the effects of atmospheric scattering, and thus judge that the broadening they observe is at best an upper limit. As a result, an airplane or balloon would provide little if any improvement in the wavelengths available for spectroscopy over an orbiter. Given these constraints, it would be difficult for a remote spectrometer to identify spectral features associated with common biological molecules on Titan.

To test this hypothesis, we obtained reflectance spectra of several molecules of biological interest in the laboratory. These include a pure powdered sample of the amino acid glycine, a pure powdered sample of the amino acid alanine, as well as a reflectance spectrum of a sample of glycine that had been dissolved in water, frozen, and desiccated under vacuum (Figure 6a). We used an ultra-high vacuum system that is able to obtain bidirectional reflectance spectra (i=0°, e=30°) using a Bruker FTIR spectrometer. The spectrometer has a typical resolution of 4 cm^{-1} (or ~10 nm at 5 μm, more than two times higher resolution than VIMS), and a wavelength range limited to ~1.8 – 5.5 μm (see Hibbitts and Szanyi, 2007).

When we compare the brightness of the laboratory spectra in the 2, 2.7, 2.8, and 5 μm atmospheric windows, we find they are almost indistinguishable from each other. They are also rather featureless, unlike water ice, which shows a prominent absorption band at 2.8 μm (Figure 6b). Moreover, given the purity of these samples, the spectra presented here represent the absolute best-case scenario for identifying biological molecules remotely. The concentration of biomolecules in cryolavas and impact melts on Titan is likely to be much lower than the concentrations measured in the laboratory. For example, hydrogen cyanide (HCN), one biomolecule precursor (Ferris et al. 1978), is produced in Titan's atmosphere at a rate of ~1.2 x 10^8 molecules cm-^{2} s^{-1} (Willacy et al. 2016). If Titan's surface is ~1 Ga old (the upper limit estimated by Neish and Lorenz, 2012), we would expect ~10^{11} moles of HCN per km^2. For a 1 km^2 region of lava or impact melt, this gives a HCN concentration of 1-10 M (for 10-100 m thick layers of water). If the yield of glycine in such a solution is ~1% (Ferris et al. 1978), we would expect glycine concentrations of only 0.01-0.1 M in the lava or impact melt. Further, the unique identification of particular molecules within a complex mixture of organics is extremely challenging even with high sensitivity, given multiple overlapping spectral features (see, for example, Clark et al., 2009).

Thus, remotely identifying biomolecules on Titan's surface from above or within Titan's atmosphere would be difficult, even with an infrared camera that has finer spatial and spectral resolution and wider spectral range than VIMS.

3.2 Detection by in-situ sampling?

Another approach for detecting biological molecules on Titan would be to sample the surface in situ. This approach would require specific measurement strategies. To date, only one spacecraft has acquired in situ information about Titan’s surface. In January 2005, the *Huygens* probe became the first (and only) spacecraft to descend through Titan’s atmosphere and land on its surface (Lebreton et al., 2005). It provided detailed information about Titan’s atmospheric profile and chemistry (Fulchignoni et al., 2005; Niemann et al., 2005), as well as information about Titan’s surface properties (Niemann et al., 2005; Tomasko et al., 2005; Zarnecki et al., 2005). The *Huygens* probe firmly identified methane and ethane, and tentatively identified cyanogen (C_2N_2), benzene (C_6H_6), and carbon dioxide (CO_2) on the surface of Titan (Niemann et al. 2010).

However, there has been as yet no identification of biological molecules on the surface of Titan, and it is unlikely that such identifications will be possible using the currently available data set. The *Huygens* probe was designed with essentially no information about Titan's surface and was not guaranteed to survive impact. As a result, it was not capable of precision landing near a site of astrobiological interest, such as an impact crater or cryovolcano. Even if it had landed in such an area, the mass resolution (1 amu) and mass range (1-140 amu) of the *Huygens* GCMS (Gas Chromatograph Mass Spectrometer) were not suited to the identification of biological molecules. Oxygenated organic molecules (e.g., $C_vH_xN_yO_z$) have mass differences much less than 1 amu compared to non-oxygenated molecules of similar molecular weight (e.g., $C_{v+1}H_{x+4}N_y$). Distinguishing between these products requires higher resolution mass spectrometers (see Neish et al, 2008; 2009; Hörst et al., 2012; Hörst, 2017) and/or a mechanism for separating different molecules with the same unit mass (Neish et al., 2010; Cleaves et al., 2014). In addition, many amino acids and nucleobases have masses in excess of 140 amu. Glutamine and glutamic acid fall into this mass range, and they represent half of the amino acids identified in one hydrolyzed sample of Titan haze analogues (Neish et al., 2010). Finally, and perhaps most importantly, the surface material sampled by GCMS did not encounter temperatures of more than ~150 K. As a result, no large complex molecules were volatilized and ingested into the instrument (Lorenz et al. 2006). The measurement of complex organics from a surface requires careful sample handling and processing to enable analysis of these molecules without degradation or conversion that obscures the chemical nature of the original material. The *Huygens* probe was not designed to perform this type of measurement.

Identification of biological molecules on Titan would require a spacecraft capable of precision landing, equipped with a payload that is designed to identify the composition and distribution of the organic molecules present within the water-ice matrix. Existing or proposed spaceflight instrumentation could be used to accomplish the in-situ detection of complex organics and potential biomolecules in the Titan surface environment. Since the deployment of the *Huygens* probe, two gas-chromatograph mass spectrometers have been flown that exploit a solid sample acquisition and processing capability to pyrolyse samples and measure a wide range of biological molecules (Goesmann et al., 2007; Mahaffy et al., 2012). Both the *Rosetta* COSAC and *Mars Science Laboratory* SAM instruments included chiral columns and derivatization agents to allow for the volatilization of key functional groups in biologically interesting molecules, such as amino acids, that would normally degrade or resist transport through the gas chromatography columns (Freissinet et al., 2010). This analysis technique has been demonstrated to successfully detect biomolecules in laboratory-based Titan organic analogs that have undergone hydrolysis (Hörst et al., 2012; Poch et al., 2012). The *ExoMars* MOMA instrument includes an additional capability of laser-desorption mass spectrometry, which may have clear advantages in diverse surface environments and for the measurement of large refractory organic molecules (Siljestrom et al., 2014; Li et al., 2015; Goesmann et al., 2017).

Sampling and measurement in organic-laden ices, as proposed here, has recently been discussed in the context of a science feasibility study of a landed Europa mission (Hand et al., 2017). With the goal of searching for signs of life, the lander's model payload includes an Organic Compositional Analyzer (OCA), baselined to be a GCMS for the detection and identification of molecular biosignatures, similar to those proposed as targets for Titan exploration. The sampling and measurement approach discussed for Europa is highly applicable to the Titan surface; in fact, the much-reduced radiation environment and anticipated high density of organic molecules eases the requirements for chemical characterization on Titan. Additional measurement approaches and sampling implementations have been discussed with respect to the challenges that are unique to cryogenic surfaces (Castillo et al., 2016).

In Section 2, we identified the highest priority targets for exploration by in situ sampling systems: the floors of large, relatively unmodified impact craters (specifically, Sinlap, Selk, and Menrva craters). Where, then, would be an ideal place to sample within these craters? Much of Titan is covered in a thick layer of organic molecules (Janssen et al., 2016), so not all impact melt deposits may be accessible on a crater floor or in its ejecta blanket. We need to identify locations where impact melt deposits have been recently exposed through erosion and/or mass wasting.

To identify an appropriate sampling site, we consider a relevant terrestrial analogue: Haughton crater in the Canadian Arctic. The 39 Ma Haughton impact structure is a well preserved 23 km diameter crater in a polar desert, with little to no obscuring vegetation (Osinski et al., 2005; Tornabene et al., 2005). Thus, it is an excellent analogue for the study of craters on worlds that have experienced moderate amounts of erosion, such as Mars or Titan. We note that the geomorphology of the crater is what makes it a good analogue; the composition of the substrate and chemical weathering experienced by the primarily carbonate rocks at Haughton would be quite different from that experienced by a water-ice-organic bedrock exposed to liquid hydrocarbons on Titan (Lorenz and Lunine, 1996). In addition, the periglacial processes that dominate the landscape in the Canadian Arctic would not be found on Titan, where the temperatures are never low enough for liquid hydrocarbons to freeze (Hanley et al., 2017).

Mapping in the interior of Haughton has revealed a large deposit of impact melt breccia in the crater floor (the light-toned materials in Figure 7a). Using geologic maps from Osinski et al. (2005), we estimate that this deposit represents ~65% of the total area of the crater floor within 5 km of the crater centre (roughly half the radius, R, of the crater), and ~20% of the crater floor within 10 km of the crater centre (roughly one crater radius). Thus, a lander would have a high probability of encountering impact melt if it were to land within ½ R of the crater centre.

Notably, this melt deposit has been incised by multiple river channels (Figure 7b), exposing fresh melt surfaces. Additional fluvial erosion and/or mass wasting then brings samples of melt to the flat, smooth, alluvial plain at the bottom of the crater (Figure 7c), where they would be easily accessible by a lander. The benefit to accessing melt deposits at the bottom of river valleys is that no drilling would be needed to reach an unaltered melt sample. Since liquid hydrocarbons do not react chemically with water ice (Lorenz and Lunine, 1996), even samples exposed to erosion and weathering in the Titan environment would remain relatively pristine. We would also not expect any major alteration due to high-energy electromagnetic radiation and/or charged particles, since ultraviolet radiation and galactic cosmic rays do not penetrate all the way to the surface of Titan (Hörst, 2017). Thus, any biological molecules present would be trapped inside the chemically inert water ice, and so should be accessible when the sample is ingested into a lander. Therefore, if we can identify river valleys on the floors of Sinlap, Selk, and Menrva impact craters, these would be ideal landing sites.

The present resolution offered by the *Cassini* RADAR instrument is insufficient to observe anything but the largest river channels; the *Huygens* probe saw many more channels near its eventual landing site than are resolved in the corresponding SAR images (e.g., Keller et al., 2008). Still, there is evidence for fluvial erosion in many of Titan's craters; for example, there is evidence for large river channels in the ejecta blankets of both Selk (Soderblom et al., 2010) and Sinlap (Neish et al., 2015). Menrva is also characterized by many large fluvial networks (Lorenz et al., 2008; Wood et al., 2010; Williams et al., 2011), which likely expose impact melt deposits in the channel walls and as riverbed sediments. Imaging from a mobile aerial platform, or perhaps from an orbiter designed to perform such measurements, could help to identify where the deposits of interest are most accessibly exposed.

In this work, we have remained agnostic as to the origin of the biological molecules we seek to find in Titan's impact craters. However, future mission planners may wish to differentiate between those biomolecules formed by abiotic processes and those formed by biotic processes. There are several indicators that may be able to differentiate between biomolecules of biotic origins from those of abiotic origins. For example, one may use isotopic signatures to differentiate between the two; life on Earth preferentially utilizes the lighter isotope of carbon, ^{12}C, over the heavier isotope, ^{13}C (Cockell, 2015). One may also look for an abundance of molecules with a single chirality; life on Earth uses only the L-stereoisomer of amino acids, and not their mirror image, the D-stereoisomer (McKay, 2016). Finally, one could consider the broader suite of molecules present in the melt pond; abiotic processes typically produce smooth distributions of organic material, while biologic processes select a highly specific set of molecules (McKay, 2004).

4. Conclusions

Biomolecules similar to those found on Earth are likely present on Titan. To identify and characterize them would require in-situ measurements of Titan's surface material, obtained through precision targeting of a lander, equipped with instrumentation capable of measuring a wide range of biological molecules. The ideal landing sites would be the floors of Titan's largest, freshest impact craters, where mass wasting and fluvial erosion expose fresh deposits of impact melt for sampling. Impact craters are preferred over cryovolcanoes for a number of reasons, chief among them the temperature of the aqueous medium; higher temperatures at impact craters will increase reaction rates exponentially, increasing the likelihood of forming complex biomolecules. Determining the extent of prebiotic chemistry within these melt deposits would help us to understand how life could originate on a world very different from Earth, and shed light on prebiotic synthesis more generally.

Acknowledgments

We wish to acknowledge the *Cassini* RADAR team for acquiring and processing the data presented here. We also wish to thank two anonymous reviewers whose comments helped to improve the manuscript. The research was supported in part by the *Cassini-Huygens* mission, a cooperative endeavor of NASA, ESA, and ASI managed by JPL/Caltech under a contract with NASA. C. N. also thanks the Canadian Space Agency and the Natural Sciences and Engineering Research Council of Canada for funds that supported field work at the Haughton impact structure. R. L. acknowledges the support of NASA PDART grant NNX15AM23G.

Author Disclosure Statement

No competing financial interests exist.

References

Artemieva, N., and Lunine, J. (2003). Cratering on Titan: impact melt, ejecta, and the fate of surface organics. *Icarus* 164:471–480.

Artemieva, N., and Lunine, J. I. (2005). Numerical calculations of the longevity of impact oases on Titan. *Icarus* 173:243–253.

Barnes, J. W., Brown, R. H., Turtle, E. P., McEwen, A. S., et al. (2005). A 5-micron-bright spot on Titan: Evidence for surface diversity. *Science* 310:92-95.

Barnes, J. W., Brown, R. H., Soderblom, L., Buratti, B. J., Sotin, C., Rodriguez, S., Baines, K. H., Clark, R., and Nicholson, P. (2007). Global-scale surface spectral variations on Titan seen from Cassini/VIMS. *Icarus* 186:242–258.

Barnes, J. W., Lemke, L., Foch, R., McKay, C. P., Beyer, R. A., Radebaugh, J., et al. (2012). AVIATR—Aerial Vehicle for In-situ and Airborne Titan Reconnaissance. A Titan airplane mission concept. *Experimental Astronomy* 33:55–127.

Béghin, C. B., Randriamboarison, O., Hamelin, M., Karkoschka, E., Sotin, C., Whitten, R. C., et al. (2012). Analytic theory of Titan's Schumann resonance: Constraints on ionospheric conductivity and buried water ocean. *Icarus* 218:1028–1042.

Bray, V. J., Schenk, P. M., Melosh, H. J., Morgan, J. V., and Collins, G. S. (2012). Ganymede crater dimensions: Implications for central peak and central pit formation and development. *Icarus* 217:115–129.

Brown, R. H., Baines, K. H., Bellucci, G., Bibring, J. P., Buratti, B. J., Capaccioni, F., et al. (2004). The Cassini visual and infrared mapping spectrometer (VIMS) investigation. *Space Science Reviews* 115:111–168.

Castillo, J. C., Y. Bar-Cohen, S. Vance, M. Choukroun, H. J. Lee, X. Bao, M. Badescu, S. Sherrit, M. G. Trainer, and S. A. Getty (2016). Sample Handling and Instruments for the In Situ Exploration of Ice-Rich Planets. In: *Low Temperature Materials and Mechanisms*, edited by Y. Bar-Cohen, CRC Press, Boca Raton, FL, pp. 229-270.

Chyba, C. et al. (1999). Europa and Titan: Preliminary Recommendations of the Campaign Science Working Group on Prebiotic Chemistry in the Outer Solar System. In: 30th *Lunar and Planetary Science Conference Abstracts*, Houston, Texas, USA.

Cintala, M. J., and Grieve, R. A. F. (1998). Scaling impact-melt and crater dimensions: Implications for the lunar cratering record. *Meteoritics & Planetary Science* 33:889–912.

Clark, R. N. (2009). Detection of Adsorbed Water and Hydroxyl on the Moon. *Science* 326:562 –564.

Clark, R.N., Curchin, J.M., Hoefen, T.M., and Swayze, G.A. (2009) Reflectance spectroscopy of organic compounds: 1. Alkanes. *Journal of Geophysical Research* 114:E03001.

Cleaves, H. J., Neish, C., Callahan, M. P., Parker, E., Fernández, F. M., and Dworkin, J. P. (2014). Amino acids generated from hydrated Titan tholins: Comparison with Miller-Urey electric discharge products. *Icarus* 237:182–189.

Cockell, C.S. (2015). *Astrobiology: Understanding life in the universe*. John Wiley & Sons, Ltd., Sussex, UK, 449 pp.

Cook-Hallett, C., J. W. Barnes, S. A. Kattenhorn, T. Hurford, J. Radebaugh, B. Stiles, and M. Beuthe (2015). Global contraction/expansion and polar lithospheric thinning on Titan from patterns of tectonism. *Journal of Geophysical Research-Planets* 120:1220–1236.

Coustenis, A., Atreya, S. K., Balint, T., Brown, R. H., Dougherty, M. K., Ferri, F., et al. (2008). TandEM: Titan and Enceladus mission. *Experimental Astronomy* 23:893–946.

Croft, S., Lunine, J., and Kargel, J. (1988). Equation of state of ammonia-water liquid: Derivation and planetological applications. *Icarus* 73:279–293.

Davies, A.G., Sotin, C., Matson, D.L., Castillo-Rogez, J., Johnson, T.V., Choukroun, M., and Baines, K.H. (2010). Atmospheric control of the cooling rate of impact melts and cryolavas on Titan’s surface. *Icarus* 208:887-895.

Ehlmann, B. L., Mustard, J. F., Murchie, S. L., Poulet, F., Bishop, J. L., Brown, A. J., et al. (2008). Orbital Identification of Carbonate-Bearing Rocks on Mars. *Science* 322:1828–1832.

El Goresy, A. (1965). Baddeleyite and its significance in impact glasses. *Journal of Geophysical Research* 70:3453–3456.

Elachi, C., et al. (2005). Cassini Radar Views the Surface of Titan. *Science* 308:970–974.

Elder, C. M., Bray, V. J., and Melosh, H. J. (2012). The theoretical plausibility of central pit crater formation via melt drainage. *Icarus* 221:831–843.

Ferris, J., Joshi, P., Edelson, E., and Lawless, J. (1978). HCN: a plausible source of purines, pyrimidines and amino acids on the primitive Earth. *Journal of Molecular Evolution* 11:293–311.

Fortes, A. (2000). Exobiological Implications of a Possible Ammonia–Water Ocean inside Titan. *Icarus* 146:444–452.

Freissinet, C., A. Buch, R. Sternberg, C. Szopa, C. Geffroy-Rodier, C. Jelinek, and M. Stambouli (2010). Search for evidence of life in space: Analysis of enantiomeric organic molecules by N,N-dimethylformamide dimethylacetal derivative dependant Gas Chromatography-Mass Spectrometry. *Journal of Chromatography A* 1217:731-740.

Fulchignoni, M., Ferri, F., Angrilli, F., Ball, A. J., Bar-Nun, A., Barucci, M. A., et al. (2005). In situ measurements of the physical characteristics of Titan's environment. *Nature* 438:785–791.

Goesmann, F., Rosenbauer, H., Roll, R., Szopa, C., Raulin, F., Sternberg, R., et al. (2007). COSAC, The Cometary Sampling and Composition Experiment on Philae. *Space Science Reviews* 128:257–280.

Goesmann, F., et al. (2017), The Mars Organic Molecule Analyzer (MOMA) Instrument: Characterization of Organic Material in Martian Sediments, *Astrobiology* 17:655-685.

Grieve, R.A.F., and Cintala, M.J. (1992). An analysis of differential impact melt-crater scaling and implications for the terrestrial impact record. *Meteoritics & Planetary Science* 27:526–538.

Hand, K.P., Murray, A.E., Garvin, J.B., Brinckerhoff, W.B., Christner, B.C, Edgett, K.S, Ehlmann, B.L., German, C.R., Hayes, A.G., Hoehler, T.M., Horst, S.M., Lunine, J.I., Nealson, K.H., Paranicas, C., Schmidt, B.E., Smith, D.E., Rhoden, A.R., Russell, M.J., Templeton, A.S., Willis, P.A., Yingst, R.A., Phillips, C.B, Cable, M.L., Craft., K.L., Hofmann, A.E., Nordheim, T.A., Pappalardo, R.P., and the Project Engineering Team (2017). *Report of the Europa Lander Science Definition Team*. Posted February, 2017.

Hanel R, Conrath B, Flasar FM, Kunde V, Maguire W, Pearl J, Pirraglia J, Samuelson R, Herath L, Allison M, Cruikshank D, Gautier D, Gierasch P, Horn L, Koppany R, Ponnamperuma C (1981). Infrared observations of the saturnian system from voyager 1. *Science* 212:192-200.

Hanley, J., Pearce, L., Thompson, G., Grundy, W., Roe, H., Lindberg, G., Dustrud, S., Trilling, D., and Tegler, S. (2017). Methane, Ethane, and Nitrogen Stability on Titan. In: *48th Lunar and Planetary Science Conference Abstracts*, The Woodlands, Texas, USA.

Hawke, B.R., and Head, J.W. (1977). Impact melt in lunar crater interiors. In: *Impact and explosion cratering*, edited by D.J. Roddy, R.O. Pepin, and R.B. Merrill, Pergamon Press, New York, NY, pp. 815.

Hayne, P. O., McCord, T. B., and Sotin, C. (2014). Titan's surface composition and atmospheric transmission with solar occultation measurements by Cassini VIMS. *Icarus* 243:158-172.

Hibbitts, C. A., and Szanyi, J. (2007). Physisorption of CO2 on nonice materials relevant to icy satellites. *Icarus* 191:371-380.

Hörst, S. M., Yelle, R. V., Buch, A., Carrasco, N., Cernogora, G., Dutuit, O., Quirico, E., Sciamma-O'Brien, E., Smith, M. A., Somogyi, A., Szopa, C., Thissen, R., and Vuitton, V. (2012). Formation of Amino Acids and Nucleotide Bases in a Titan Atmosphere Simulation Experiment. *Astrobiology* 12:809–817.

Hörst, S. M. (2017). Titan's atmosphere and climate. *Journal of Geophysical Research-Planets* 122:432–482.

Hörz F. (1965). Untersuchungen an Riesgläsern, *Beiträge zur Mineralogie und Petrographie* 11:621–661.

Iess, L., Jacobson, R. A., Ducci, M., Stevenson, D. J., Lunine, J. I., Armstrong, J. W., et al. (2012). The Tides of Titan. *Science* 337:457–459.

Ivanov, B. A., Basilevsky, A. T., and Neukum, G. (1997). Atmospheric entry of large meteoroids: implication to Titan. *Planetary and Space Science* 45:993–1007.

Jankowski, D., and Squyres, S. (1988). Solid-State Ice Volcanism on the Satellites of Uranus. *Science* 241:1322–1325.

Janssen, M. A., Le Gall, A., Lopes, R. M., Lorenz, R. D., Malaska, M. J., Hayes, A. G., et al. (2016). Titan's surface at 2.18-cm wavelength imaged by the Cassini RADAR radiometer: Results and interpretations through the first ten years of observation. *Icarus* 270:443–459.

Jones, K. B., Head, J. W., III, Pappalardo, R. T., and Moore, J. M. (2003). Morphology and origin of palimpsests on Ganymede based on Galileo observations. *Icarus* 164:197–212.

Keller, H. U., Grieger, B., Küppers, M., Schröder, S. E., Skorov, Y. V., and Tomasko, M. G. (2008). The properties of Titan's surface at the Huygens landing site from DISR observations. *Planetary and Space Science* 56:728–752.

Kirchoff, M.R. and Schenk, P. (2010). Impact cratering records of the mid-sized, icy saturnian satellites. *Icarus* 206:485-497.

Korycansky, D. G., and Zahnle, K. J. (2005). Modeling crater populations on

Venus and Titan. *Planetary and Space Science* 53:695–710.

Kraus, R. G., Senft, L. E., and Stewart, S. T. (2011). Impacts onto H2O ice: Scaling laws for melting, vaporization, excavation, and final crater size. *Icarus* 214:724–738.

Kunde, V. G., Aikin, A. C., Hanel, R. A., and Jennings, D. E. (1981). C4H2, HC3N and C2N2 in Titan's atmosphere. *Nature* 292:686-688.

Lavvas, P. P., Coustenis, A., and Vardavas, I. M. (2008). Coupling photochemistry with haze formation in Titan's atmosphere, Part II: Results and validation with Cassini/Huygens data. *Planetary and Space Science* 56:67-99.

Lebreton, J.-P., Witasse, O., Sollazzo, C., Blancquaert, T., Couzin, P., Schipper, A.-M., et al. (2005). An overview of the descent and landing of the Huygens probe on Titan. *Nature* 438:758–764.

Li, X., R. M. Danell, W. B. Brinckerhoff, V. T. Pinnick, F. van Amerom, R. D. Arevalo, S. A. Getty, P. R. Mahaffy, H. Steininger, and F. Goesmann (2015). Detection of Trace Organics in Mars Analog Samples Containing Perchlorate by Laser Desorption/Ionization Mass Spectrometry. *Astrobiology* 15:104-110.

Liu, Z.Y.C., Radebaugh, J., Christiansen, E.H., Harris, R.A., Neish, C.D., Kirk, R.L. and Lorenz, R.D. (2016) The tectonics of Titan: Global structural mapping from Cassini RADAR. *Icarus* 270:14-29.

Lopes, R. M. C., Kirk, R. L., Mitchell, K. L., Legall, A., Barnes, J. W., Hayes, A., et al. (2013). Cryovolcanism on Titan: New results from Cassini RADAR and VIMS. *Journal of Geophysical Research-Planets* 118:416–435.

Lorenz, R.D. (2000) Post-Cassini Exploration of Titan: Science Rationale and Mission Concepts. *Journal of the British Interplanetary Society* 53:218-234.

Lorenz, R., and Mitton, J. (2002). *Lifting Titan's Veil*. Cambridge University Press, Cambridge, UK, 260 pp.

Lorenz, R. D., and Lunine, J. I. (1996). Erosion on Titan: Past and present. *Icarus* 122:79–91.

Lorenz, R. D., Niemann, H., Harpold, D., and Zarnecki, J. (2006). Titan's Damp Ground: Constraints on Titan Surface Thermal Properties from the Temperature Evolution of the Huygens GCMS inlet. *Meteoritics and Planetary Science*

41:1405-1414.

Lorenz, R. D., Lopes, R. M., Paganelli, F., Lunine, J. I., Kirk, R. L., Mitchell, K. L., et al. (2008). Fluvial channels on Titan: Initial Cassini RADAR observations. *Planetary and Space Science* 56:1132–1144.

Lorenz, R. D., Stofan, E., Lunine, J. I., Zarnecki, J. C., Harri, A. M., Karkoschka, E., et al. (2012). MP3 - A meteorology and physical properties package to explore air-sea interaction on Titan. In: 43rd *Lunar and Planetary Science Conference Abstracts*, Houston, Texas, USA.

Maguire, W. C., Hanel, R. A., Jennings, D. E., and Kunde, V. G. (1981). C3H8 and C3H4 in Titan's atmosphere. *Nature* 292:683–686.

Mahaffy, P. R., Webster, C. R., Cabane, M., Conrad, P. G., Coll, P., Atreya, S. K., et al. (2012). The Sample Analysis at Mars Investigation and Instrument Suite. *Space Science Reviews* 170:401–478.

McDonald, G.D., Corlies, P., Wray, J.J., Horst, S.M., Hofgartner, J.D., Liuzzo, L.R., Buffo, J., and Hayes, A. G. (2015). Altitude-dependence of Titan's methane transmission windows: Informing future missions. In: 46th *Lunar and Planetary*

Science Conference Abstracts, The Woodlands, Texas, USA.

McKay, C. P. (2004). What Is Life—and How Do We Search for It in Other Worlds? *PLoS Biology*, 2:e302–4.

McKay, C. P. (2016). Titan as the Abode of Life. *Life* 6:8.

Mitri, G., Showman, A., Lunine, J., and Lopes, R. (2008). Resurfacing of Titan by ammonia-water cryomagma. *Icarus* 196:216–224.

Mitri, G., Meriggiola, R., Hayes, A., Lefèvre, A., Tobie, G., Genova, A., et al. (2014). Shape, topography, gravity anomalies and tidal deformation of Titan. *Icarus* 236:169–177.

Moore, J. M., and Pappalardo, R. T. (2011). Titan: An exogenic world? *Icarus* 212:790–806.

Neish, C. D., and Lorenz, R. D. (2012). Titan’s global crater population A new assessment. *Planetary and Space Science* 60:26–33.

Neish, C. D., and Lorenz, R. D. (2014). Elevation distribution of Titan's craters suggests extensive wetlands. *Icarus* 228:27-34.

Neish, C. D., Lorenz, R. D., O'Brien, D. P., and the Cassini RADAR Team. (2006). The potential for prebiotic chemistry in the possible cryovolcanic dome Ganesa Macula on Titan. *International Journal of Astrobiology* 5:57-65.

Neish, C. D., Somogyi, Á., Imanaka, H., Lunine, J. I., and Smith, M. A. (2008). Rate Measurements of the Hydrolysis of Complex Organic Macromolecules in Cold Aqueous Solutions: Implications for Prebiotic Chemistry on the Early Earth and Titan. *Astrobiology* 8:273–287.

Neish, C. D., Somogyi, Á., Lunine, J. I., and Smith, M. A. (2009). Low temperature hydrolysis of laboratory tholins in ammonia-water solutions: Implications for prebiotic chemistry on Titan. *Icarus* 201:412–421.

Neish, C. D., Somogyi, Á., and Smith, M. A. (2010). Titan's Primordial Soup: Formation of Amino Acids via Low-Temperature Hydrolysis of Tholins. *Astrobiology* 10:337–347.

Neish, C. D., Kirk, R. L., Lorenz, R. D., Bray, V. J., Schenk, P., Stiles, B. W., et al. (2013). Crater topography on Titan: Implications for landscape evolution.

Icarus 223:82–90.

Neish, C. D., Barnes, J. W., Sotin, C., MacKenzie, S., Soderblom, J. M., Le Mouélic, S., et al. (2015). Spectral properties of Titan’s impact craters imply chemical weathering of its surface. *Geophysical Research Letters* 42:3746-3754.

Neish, C. D., Molaro, J. L., Lora, J. M., Howard, A. D., Kirk, R. L., Schenk, P., et al. (2016). Fluvial erosion as a mechanism for crater modification on Titan. *Icarus* 270:114–129.

Neish, C. D., Herrick, R. R., Zanetti, M., and Smith, D. (2017). The role of pre-impact topography in impact melt emplacement on terrestrial planets. *Icarus* 297:240–251.

Niemann, H. B., Atreya, S. K., Bauer, S. J., Carignan, G. R., Demick, J. E., Frost, R. L., et al. (2005). The abundances of constituents of Titan's atmosphere from the GCMS instrument on the Huygens probe. *Nature* 438:779–784.

Niemann, H. B., Atreya, S. K., Demick, J. E., Gautier, D., Haberman, J. A., Harpold, D. N., Kasprzak, W. T., Lunine, J. I., Owen, T. C., and Raulin, F. (2010). Composition of Titan’s lower atmosphere and simple surface volatiles as measured by the Cassini-Huygens probe gas chromatograph mass spectrometer experiment. *Journal of Geophysical Research* 115:E12006.

Nimmo, F., and Bills, B. G. (2010). Shell thickness variations and the long-wavelength topography of Titan. *Icarus* 208:896–904.

O'Brien, D. P., Lorenz, R. D., and Lunine, J. I. (2005). Numerical calculations of the longevity of impact oases on Titan. *Icarus* 173:243–253.

Osinski, G. R., Lee, P., Parnell, J., and Spray, J. G. (2005). A case study of impact-induced hydrothermal activity: The Haughton impact structure, Devon Island, Canadian High Arctic. *Meteoritics & And Planetary Science* 40:1859-1877.

Osinski, G.R., Grieve, R.A.F., Bleacher, J.E., Pilles, E.A., and Tornabene, L.L. (2017) Igneous rocks formed by hypervelocity impact. *Journal of Volcanological and Geothermal Research* submitted.

Pierazzo, E., Vickery, A. M., and Melosh, H. J. (1997). A Reevaluation of Impact Melt Production. *Icarus* 127:408–423.

Pieters, C. M., Goswami, J. N., Clark, R. N., Annadurai, M., Boardman, J., Buratti, B., et al. (2009). Character and Spatial Distribution of OH/H2O on the Surface of the Moon Seen by M3 on Chandrayaan-1. *Science* 326:568–572.

Pilcher, C. B., Ridgway, S. T., and McCord, T. B. (1972). Galilean Satellites: Identification of Water Frost. *Science* 178:1087–1089.

Poch, O., Coll, P., Buch, A., Ramírez, S. I., and Raulin, F. (2012). Production yields of organics of astrobiological interest from H2O–NH3 hydrolysis of Titan's tholins. *Planetary and Space Science* 61:114–123.

Porco, C. C., Baker, E., Barbara, J., Beurle, K., Brahic, A., Burns, J. A., et al. (2005). Imaging of Titan from the Cassini spacecraft. *Nature* 434:159–168.

Porco, C. C., Helfenstein, P., Thomas, P. C., Ingersoll, A. P., Wisdom, J., West, R., et al. (2006). Cassini Observes the Active South Pole of Enceladus. *Science* 311:1393–1401.

Richardson, J., Lorenz, R. D., and McEwen, A. (2004). Titan's surface and rotation: new results from Voyager 1 images. *Icarus* 170:113-124.

Roth, L., Retherford, K. D., Saur, J., Strobel, D. F., Feldman, P. D., McGrath, M. A., and Nimmo, F. (2014). Orbital apocenter is not a sufficient condition for HST/STIS detection of Europa's water vapor aurora. *Proceedings of the National Academy of Sciences* 111:E5123–E5132.

Schenk, P. M. (2002). Thickness constraints on the icy shells of the galilean satellites from a comparison of crater shapes. *Nature* 417:419–421.

Schulze-Makuch, D., and Grinspoon, D. (2005). Biologically enhanced energy and carbon cycling on Titan? *Astrobiology* 5:560–567.

Showman, A. P., Mosqueira, I., and Head, J. W., III. (2004). On the resurfacing of Ganymede by liquid–water volcanism. *Icarus* 172:625–640.

Siljestrom, S., C. Freissinet, F. Goesmann, H. Steininger, W. Goetz, A. Steele, H. Amundsen, and the AMASE11 Team (2014). Comparison of Prototype and Laboratory Experiments on MOMA GCMS: Results from the AMASE11 Campaign. *Astrobiology* 14:780-797.

Simonds, C.H., Warner, J.L., and Phinney, W.C. (1976). Thermal regimes in cratered terrain with emphasis on the role of impact melt. *American Mineralogist*

61:569–577.

Soderblom, J. M., Brown, R. H., Soderblom, L. A., Barnes, J. W., Jaumann, R., Le Mouélic, S., et al. (2010). Geology of the Selk crater region on Titan from Cassini VIMS observations. *Icarus* 208:905–912.

Space Studies Board (2012). Vision and Voyages for Planetary Science in the Decade 2013–2022. National Academies Press. Available online at http://solarsystem.nasa.gov/docs/Vision_and_Voyages-FINAL.pdf.

Sparks, W.B., Schmidt, B.E., McGrath, M.A., Hand, K.P., Spencer, J.R., Cracraft, M., and Deustua, S.E. (2017). Active Cryovolcanism on Europa? *Astrophysical Journal Letters* 839:L18.

Stiles, B. W., Hensley, S., Gim, Y., Bates, D. M., Kirk, R. L., Hayes, A., et al. (2009). Determining Titan surface topography from Cassini SAR data. *Icarus* 202:584–598.

Stofan, E., Lorenz, R. D., Lunine, J. I., Bierhaus, E. B., Clark, B., Mahaffy, P.R., Ravine, M. (2013). TiME–The Titan Mare Explorer. In: *Proceedings of IEEE Aerospace Conference*, Big Sky, MT, March 2013, paper #2434.

Sunshine, J. M., Farnham, T. L., Feaga, L. M., Groussin, O., Merlin, F., Milliken, R. E., and A'Hearn, M. F. (2009). Temporal and Spatial Variability of Lunar Hydration As Observed by the Deep Impact Spacecraft. *Science* 326:565–568.

Thompson, W.R. and Sagan, C. (1992). Organic chemistry on Titan: surface interactions. In: *Proceedings of the Symposium on Titan*, 9–12 September 1991, Toulouse, France. ESA SP-338, pp. 167–176.

Tobie, G., Grasset, O., Lunine, J. I., Mocquet, A., and Sotin, C. (2005). Titan's internal structure inferred from a coupled thermal-orbital model. *Icarus* 175:496–502.

Tomasko, M. G. (1980). Preliminary results of polarimetry and photometry of Titan at large phase angles from Pioneer 11. *Journal of Geophysical Research: Space Physics* 85:5937–5942.

Tomasko, M. G., Archinal, B., Becker, T., Bézard, B., Bushroe, M., Combes, M., et al. (2005). Rain, winds and haze during the Huygens probe's descent to Titan's surface. *Nature* 438:765–778.

Tornabene, L. L., Moersch, J. E., Osinski, G. R., Lee, P., and Wright, S. P. (2005). Spaceborne visible and thermal infrared lithologic mapping of impact-exposed subsurface lithologies at the Haughton impact structure, Devon Island, Canadian High Arctic: Applications to Mars. *Meteoritics & Planetary Science* 40:1835–1858.

Trainer, M. G., Mahaffy, P. R., Stofan, E. R., Lunine, J. I., and Lorenz, R. D. (2012). Measuring the Composition of a Cryogenic Sea. *International Workshop on Instrumentation for Planetary Missions* 1683:1033.

Willacy, K., Allen, M. and Yung, Y. (2016). A new astrobiological model of the atmosphere of Titan. *The Astrophysical Journal* 829:79.

Williams, D.A., Radebaugh, J., Lopes, R.M.C., and Stofan, E. (2011) Geomorphologic mapping of the Menrva region of Titan using *Cassini* RADAR data. *Icarus* 212:744-750.

Wood, C. A., Lorenz, R., Kirk, R., Lopes, R., Mitchell, K., and Stofan, E. (2010). Impact craters on Titan. *Icarus* 206:334–344.

Yung, Y. L., Allen, M., and Pinto, J. P. (1984). Photochemistry of the atmosphere of Titan - Comparison between model and observations. *Astrophysical Journal Supplement Series* 55:465–506.

Zahnle, K., Schenk, P., Levison, H., and Dones, L. (2003). Cratering rates in the outer Solar System. *Icarus* 163:263–289.

Zarnecki, J. C., Leese, M. R., Hathi, B., Ball, A. J., Hagermann, A., Towner, M. C., et al. (2005). A soft solid surface on Titan as revealed by the Huygens Surface Science Package. *Nature* 438:792–795.

Tables

Table 1: Relative depths for seven 'certain' or 'nearly certain' craters on Titan with D > 75 km.

Crater	Diameter, D (km)	Depth, d (m)	Technique	Relative depth, R[a]	Relative depth, R[c]	Source of Depth Measurement
Soi	78 ± 2	240 ± 120	Stereo	0.78 ± 0.11	0.76 ± 0.12	Neish et al. (2015)
Selk	79 ± 7	470 ± 90	SARTopo	0.58 ± 0.08	0.53 ± 0.09	This paper
Sinlap	82 ± 2	640 (+160/-150)	SARTopo	0.43 (+0.14/-0.13)	0.36 (+0.16/-0.15)	Neish et al. (2013)
Hano	100 ± 5	420 ± 40	SARTopo	0.65 ± 0.03	0.56 ± 0.04	This paper
		~0	Stereo	~1	~1	This paper
Afekan	115 ± 5	455 (+175/-180)	SARTopo	0.62 (+0.15/-0.15)[b]	0.52 (+0.19/-0.19)	Neish et al. (2013)
Forseti	140 ± 10	180 ± 60	Stereo	0.85 ± 0.05[b]	0.80 ± 0.07	This paper
		>410 ± 50	SARTopo	< 0.66 ± 0.04[b]	< 0.55 ± 0.06	This paper
Menrva	425 ± 25	490 (+110/-120)	SARTopo	N/A	N/A	Neish et al. (2013)

[a]Ganymede crater depths from Table 4 in Bray *et al*. (2012).

[b]Assumed to have the same depth as a D = 100 km crater.

[c]Ganymede crater depths from Figure 2b in Schenk (2002).

Figures

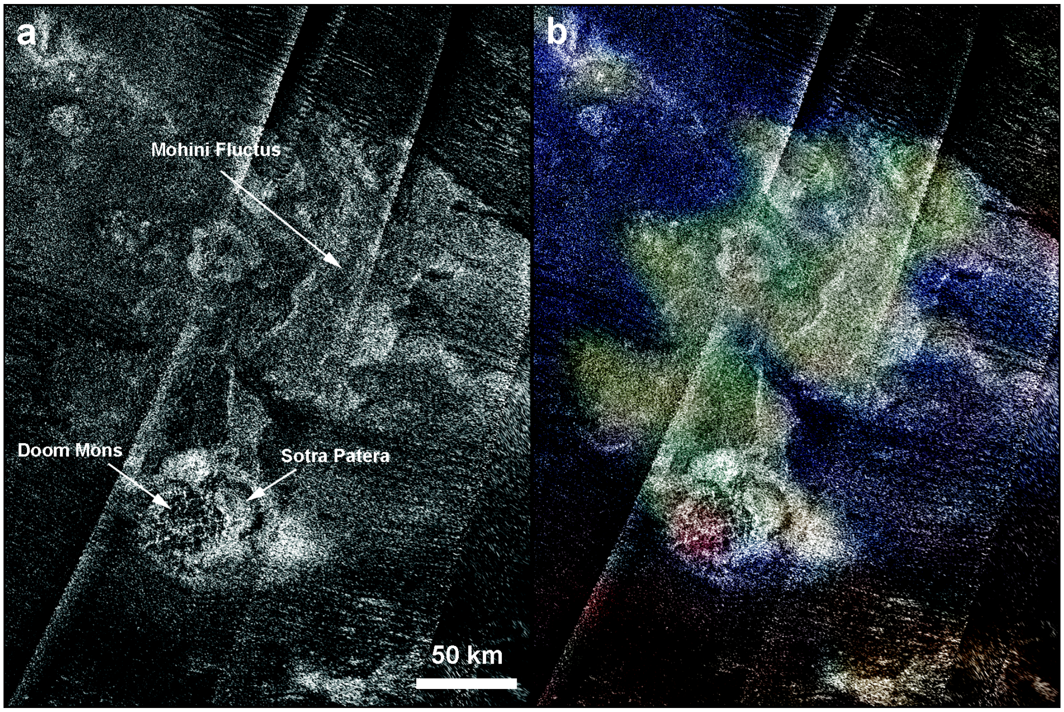

FIG. 1. (a) *Cassini* RADAR image of Sotra Facula (centered near 13°S, 40°E). Sotra Patera (a 1700 m deep pit), Doom Mons (a 1450 m high mountain), and Mohini Fluctus (flow-like features tens of meters high) are labeled. **(b)** *Cassini* VIMS image of Sotra Facula, overlaid on the *Cassini* RADAR image (R: average over 4.90 to 5.07 μm, G: 2.02 μm, B: 1.28 μm). The dune fields are ‘brown’ in colour and ‘blue’ regions may be enriched in water ice. The ‘yellowish-green’ regions have an unknown composition, but may be a combination of water ice and organic molecules (Neish et al., 2015).

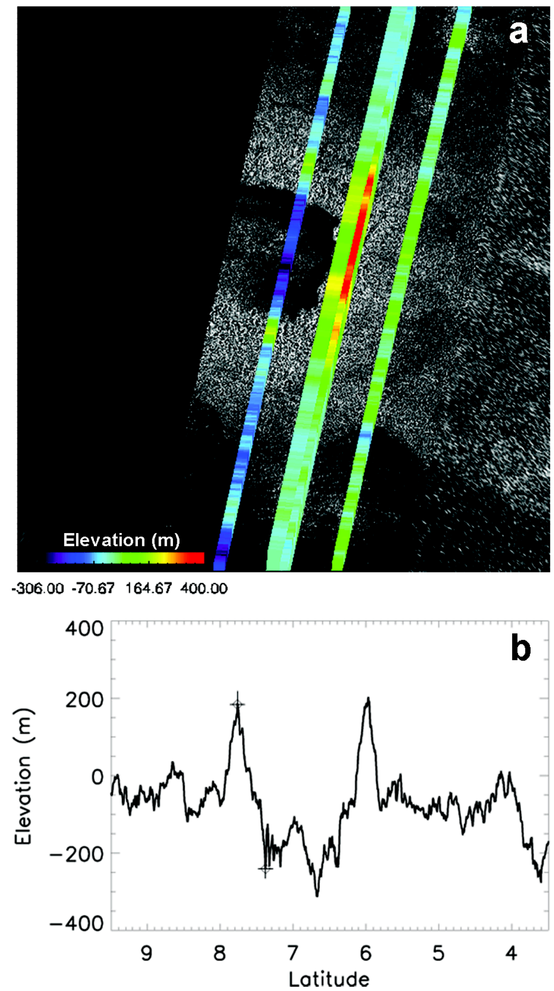

FIG. 2. (a) SARTopo profiles overlain on a *Cassini* RADAR image of Selk crater. The colours refer to the relative height at any point. North is up, and the image covers the range 3.5 – 9.5°N, 196 – 202°W. **(b)** The westernmost SARTopo profile from (a). Crosses indicate the points used to determine the depth of the northern half of the crater, d_1. Similar depth measurements were made in the southern half of the crater.

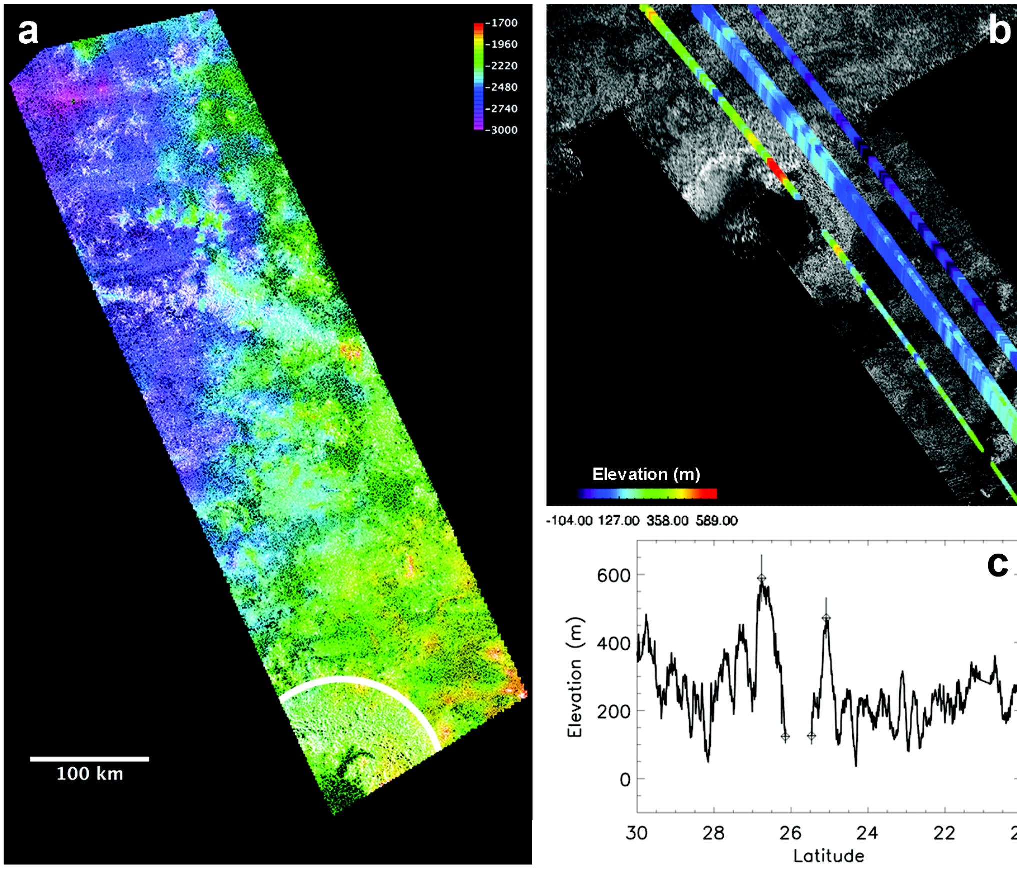

FIG. 3. (a) Stereo topography of Forseti crater in the overlapping region of the T23 and T84 passes, overlain on a *Cassini* RADAR image. The crater is outlined at bottom left. **(b)** SARTopo profiles overlaid on a *Cassini* RADAR image of Forseti crater. The colours refer to the relative height at any point. North is up, and the image covers the range 20 – 30°N, 5 – 15°W. **(c)** The westernmost SARTopo profile from (a). Crosses indicate the points used to determine the minimum depth of the crater.

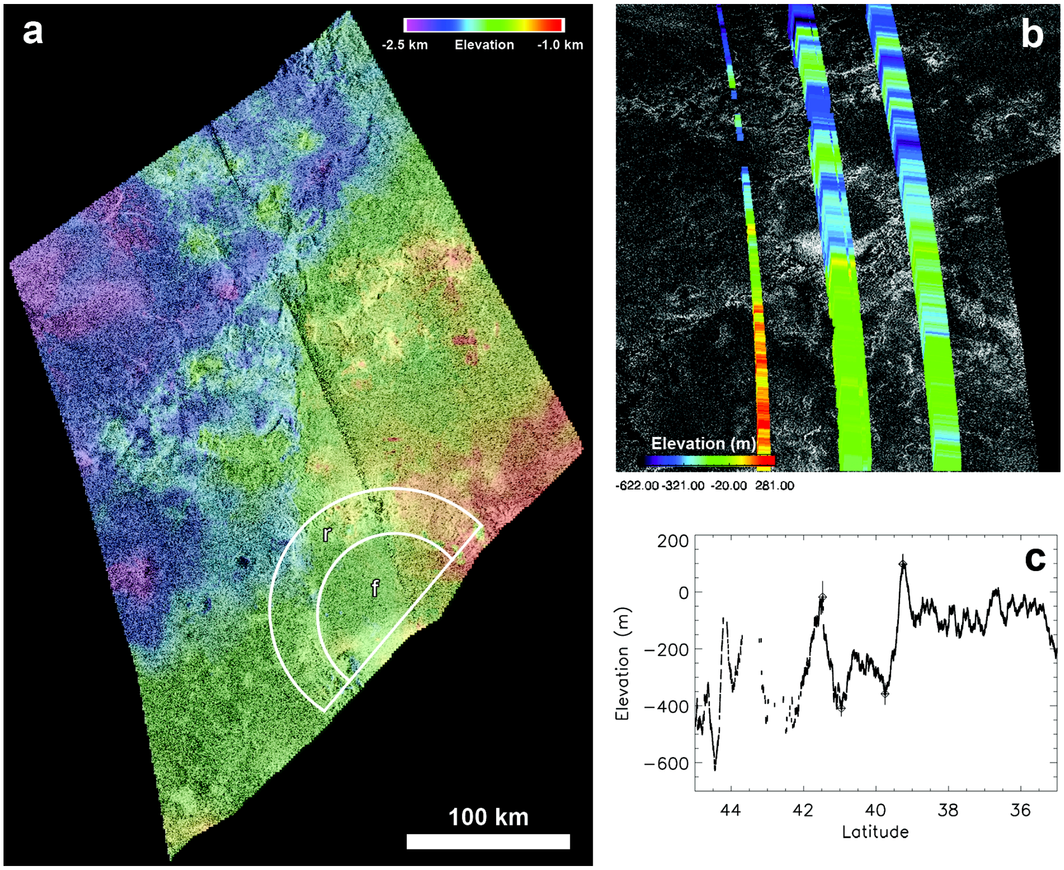

FIG. 4. (a) Stereo topography of Hano crater in the overlapping region of the T16 and T84 passes, overlain on a *Cassini* RADAR image. The regions of Hano crater used to estimate the floor elevation (f) and rim elevation (r) are outlined at the bottom. **(b)** SARTopo profiles overlaid on a *Cassini* RADAR image of Hano crater. The colours refer to the relative height at any point. North is up, and the image covers the range 35 – 45°N, 340 – 350°W. **(c)** The center SARTopo profile from (a). Crosses indicate the points used to determine the depth of the crater.

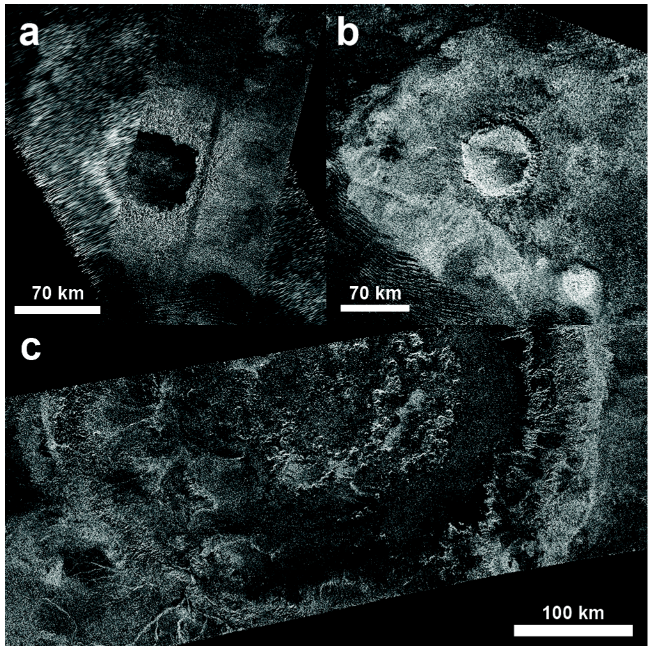

FIG. 5. These three large, relatively unmodified impact craters on Titan would be the best locations to identify biological molecules on its surface: **(a)** The 79 ± 7 km diameter Selk (7°N, 198°W), **(b)** the 82 ± 2 km diameter Sinlap (11°N, 16°W), (b) and **(c)** the 425 ± 25 km diameter Menrva (20°N, 87°W).

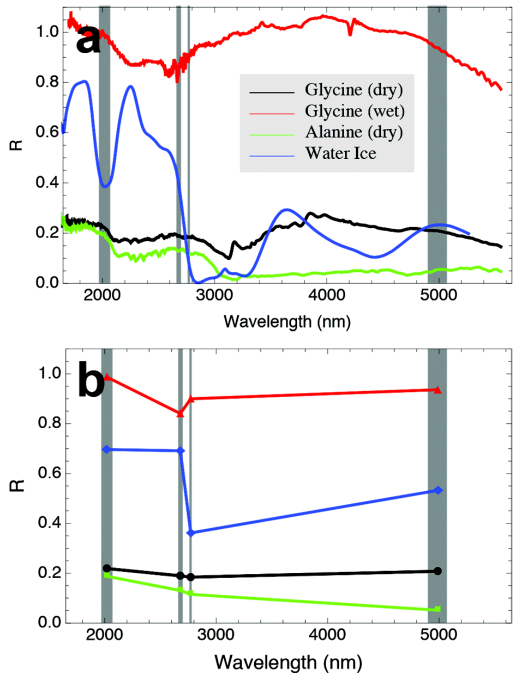

FIG. 6. (a) Reflectance spectrum of powdered glycine (black), powdered alanine (green), pure water ice (blue), and glycine dissolved in water, frozen, and later warmed and desiccated under vacuum (red). Spectra of the amino acids have been obtained at both 100 K and room temperature, and they are identical for these materials. Shown in grey are the spectral windows through which VIMS can observe surface features on Titan. (Note that the 3.1-μm feature in the spectrum of dry glycine is due to water-ice build-up in the cryogenic infrared detector.) **(b)** Spectra of water ice (blue), "dry" glycine (black), "dry" alanine (green), and "wet" glycine (red) sampled in the four long-wavelength Titan atmospheric windows. The water-ice spectrum has been shifted vertically by 0.3 for ease of viewing.

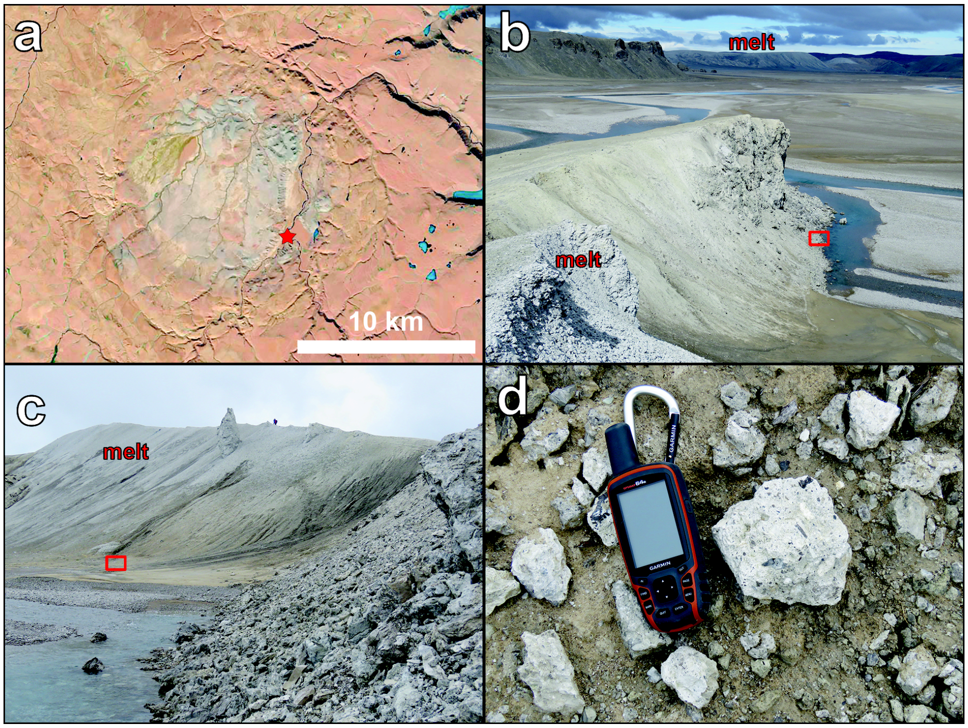

FIG. 7. (a) Landsat-8 Operational Land Imager (OLI) natural colour image of Haughton crater (75.4°N, 89.7°W) on Devon Island, Nunavut, Canada. The star indicates the location of (b). North is up. **(b)** Lighter toned impact melt has been exposed by the erosion of the impact crater interior by the Haughton River. View is to the north. The box indicates the location where the author photographed image (c). **(c)** Mass wasting and fluvial erosion brings samples of impact melt breccia into the smooth river valley bottom. View is to the south, and a person is visible on the ridgeline for scale. The box indicates the location where the author photographed image (d). **(d)** If craters on Titan are similar in morphology to Haughton, samples such as this ~10-cm cobble of impact melt breccia would be safely accessible by a lander on the flat floor of a river valley.